*Manuscript
Click here to view linked References

**The published version of the paper "Meniconi, S., Brunone, B., Ferrante M., and Capponi C. (2016). Mechanism of interaction of pressure waves at a discrete blockage. Journal of Fluids and Structures, 62, 33-45." is available at: https://doi.org/10.1016/j.jfluidstructs.2015.12.010**

# Mechanism of interaction of pressure waves at a discrete partial blockage

Silvia Meniconi, Bruno Brunone, Marco Ferrante, Caterina Capponi

*Dipartimento di Ingegneria Civile ed Ambientale, University of Perugia, via G. Duranti 93, 06125 Perugia, Italy*

## Abstract

This paper analyses the mechanism of interaction between an incident pressure wave and blockages of different geometrical characteristics (i.e., a butterfly and a ball valves, two short stretches of pipe with a reduced diameter, and a device simulating a longitudinal body blockage) by means of laboratory and numerical tests. Experiments have shown that the mechanism of interaction with pressure waves is influenced by their path through the device: sinuous because of the device body for partially closed in-line valves (type I mechanism), and straight for the small bore pipe devices (type II mechanism). Type I mechanism is characterized by a rise followed by an almost constant value whereas in type II one a drop occurs after the rise. To complete the investigation the effect of the pre-transient condition is discussed.

*Keywords:* Partial blockage, Transient tests, Pipe diagnosis, Pressure waves, In-line valves

## 1. Introduction

Partial blockages in pipelines are an important operational problem since they reduce flow, cause local low pressure values and increase pumping costs. Moreover they deteriorate water quality since they give a better chance of survival to different microorganisms serving as a food source as well as facilitating their interaction (Boulos et al., 2006; Douterelo et al., 2014). "Natural" partial blockages can be due to slow processes of deposition of chemicals in the oil industry or excess calcium carbonate scale in water pipelines (e.g., those fed by wells) whereas negligence in system maintenance is the cause of unintended partially closed valves ("artificial" partial blockage).

Within the variety of faults affecting real pipelines, partial blockages can be considered among the most insidious ones since no external evidence allows their detection. As a consequence, reliable, non-intrusive and fast techniques for partial blockage (hereafter referred to simply as blockage) detection are of great interest. The analysis and benchmarking of the available methods for blockage detection are beyond the scope of this paper that concerns with those based on the transient pressure response of pipelines, i.e. on the interaction between injected pressure waves and blockages. Last decade literature on this topic has analyzed the role played by the characteristics of such features – length and severity – on their transient behavior mostly for single pipes. For a given severity, the distinction between discrete and extended blockages is based on the significant frequency shift in the pressure signal (i.e., the pressure time-history) caused by the latter with respect to clear (i.e., blockage-free) pipes. On the contrary, no perceptible frequency shifts can be observed in pipes with discrete blockages as well as partially closed in-line valves (Lee et al., 2008; Lee and Vitkovsky, 2008). In other words, when the blockage can be approximated as a localized discontinuity in the system it is referred to as a discrete blockage whereas extended blockages occur when significant stretches of pipe are affected by the constriction (Brunone et al., 2008a; Duan et al., 2012).

Irrespective of blockage characteristics, the analysis of the pressure signal can be executed both in the frequency- (Lee et al., 2013) and time-domain (Meniconi et al., 2011a). More recently, a coupled frequency- and time-domain approach has been proposed (Meniconi et al., 2013b) and the wave scattering effect of rough blockages has been examined in the laboratory (Duan et al., 2014c). A totally different approach has been proposed by Massari et al. (2013, 2014, 2015) where the stochastic Successive Linear Estimator (SLE) – extended from groundwater hydrology (Yeh et al., 1996) – is used to infer the presence of extended partial blockages casting the inverse problem of the diagnosis in the probabilistic framework.

Frequency response techniques have been used by Mohapatra et al. (2006a,b); Mohapatra and Chaudhry (2011); Sattar et al. (2008) to point out the impact of discrete blockages in terms of the amplitude of odd and even harmonics when sinusoidal oscillations are used to excite the system (Chaudhry, 2014). Frequency, phase, and amplitude of the blockage-induced pattern – with transients generated by operating a side-discharge valve – are quantified in Lee et al. (2008) where a simple analytical expression is also proposed. The so obtained frequency response diagrams (FRD) can be used as look-up charts within the diagnosis procedure (Lee and Vitkovsky, 2008). A blockage detection method using blockage-induced pressure damping is proposed by Wang et al. (2005); a discussion in terms of total kinetic and internal energies (Karney, 1990) of such a method is offered in Meniconi et al. (2014). The case of extended blockages is examined by Duan et al. (2012, 2013, 2014a) where it is shown that, as mentioned above, the effect of blockages is a change of the resonant frequencies of the system and then the phase shift of the frequency peaks is used to detect and locate blockages. It is also demonstrated and checked by means of both numerical and laboratory experiments that friction does not affect the resonant peak frequencies as well as the assumed linear behavior of pipe connection junctions. On the contrary, the effects of viscoelasticity of pipe material must be isolated and removed from the data before executing the diagnosis. It is also pointed out that the location and length of the blockages can be detected to a greater accuracy than its severity. In a more recent paper (Duan et al., 2014b), the reasons of the blockage-induced shift in the system resonant frequencies are investigated by means of a wave perturbation analysis. In this paper, an analytical relationship between the blockage characteristics and the resonant frequency shift is given.

When the pressure signal is examined in the time-domain, attention is focused on the pressure wave reflected by the blockage: in fact, the capture of the instant of time when it reaches the measurement section allows locating the blockage whereas its magnitude derives from blockage severity. More precisely, for a given incident pressure wave, the larger the local head loss through the discrete blockage, the larger the reflected pressure wave (Contractor, 1965; Brunone et al., 2008b; Meniconi et al., 2010, 2011a). Within such an approach, in the case of extended blockages, the double reflection caused by the reduction and subsequent enlargement can be easily detected in the pressure signal (Brunone et al., 2008a). Turning points of numerical simulations of transients in pipes with a blockage by current methods – e.g., the method of the characteristics – have been highlighted for both gas (Adewumi et al., 2000, 2003) and fluid flow (Meniconi et al., 2012a; Tuck et al., 2013).

The above brief literature review shows that in the last decade of intense research activity, attention has been focused mainly on the distinction between discrete and extended blockages in terms of the induced-or-not time shift and magnitude of reflected pressure waves within the frequency- and time-domain approach, respectively. Some attention has been also devoted

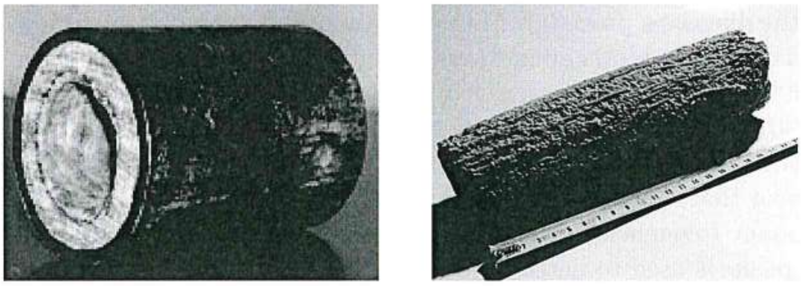

(a) (b)

Figure 1: Different shapes of real pipe discrete blockages: a) internal pipe diameter reduction (often in metallic pipes); b) longitudinal body (often in plastic pipes).

to the analysis of test conditions – pointing out the importance of the characteristics of the generated pressure waves (Lee et al., 2008; Brunone et al., 2008b) – and the negligible influence of the geometry of the section area changes between clear and blocked stretches of pipe in the case of extended blockages (Meniconi et al., 2012a).
Based on real pipe experience where different blockage features happen according to pipe material – i.e., a quite regular diameter reduction for metallic pipes (Fig. 1a) and longitudinal bodies for plastic pipes (Fig. 1b) – the aim of this paper is to analyze the mechanism of interaction between the incident pressure waves and a discrete blockage with different geometrical characteristics. In such a context, laboratory and numerical tests have been executed to examine the transient behavior of different devices (i.e., a butterfly and a ball valve, two short stretches of pipe with a reduced diameter, and a device simulating a longitudinal body blockage).

## 2. Laboratory set-up

The laboratory set-up at the Water Engineering Laboratory (WEL) of the University of Perugia, Italy, consists of a high density polyethylene (HDPE) pipe (length, $L$ = 164.93 m, internal diameter, $D$ = 93.3 mm, and wall thickness $e$ = 8.1 mm) supplied by a pressurized tank (T); pressure waves are generated by the complete and fast closure of the maneuver valve (V) installed at the downstream end section (Fig. 2) of the pipe.
During transient tests, the pressure signal (i.e., the pressure time-history), $H$, has been measured at a section placed 0.6 m upstream of the maneuver

valve (section M in Fig. 2) by means of a piezoresistive transducer (2200 series by Gems), with a different full scale according to the maximum measured pressure value, and a sampling frequency of 1024 Hz. The steady-state mean flow velocity, $V_0$, and local head loss across the blockage, $\zeta_{ID,0}$, have been measured by means of a magnetic flow meter (ML210 by Isoil) and a variable reluctance differential pressure transducer (DP15 by Validyne), respectively; the subscripts $ID$ and 0 indicate the in-line device and the pre-transient condition, respectively. During tests the water temperature (at average equal to 20°C) has been measured by a digital resistance thermometer (TRI by Gefran) and then, the related kinematic viscosity, $\nu$, and fluid density, $\rho$ have been evaluated ($\nu = 1.003\ 10^{-6}$ m$^2$/s and $\rho = 998.21$).
The in-line device simulating the discrete blockage is placed at a distance $L_2 = 75.97$ m upstream of the valve V. Five types of blockages are considered in this study: a ball (BV, PN35 by Tecnovielle) and a butterfly valve (BTV, PN16 by InterApp), which simulate "artificial" features, a small bore pipe (SBP), a very short stretch of pipe (hereafter referred to as *very short blockage*, VSB, Fig. 3), and a longitudinal body blockage (LB, Fig. 4), which simulate "natural" features.

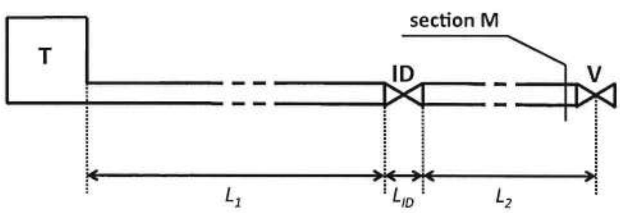


Figure 2: Experimental set-up (T = supply tank, ID = in-line device simulating the discrete blockage, M = measurement section, and V = maneuver valve).

The characteristics of such devices – length, $L_{ID}$, and diameter, $D_{ID}$ – are reported in Table 2 where $D_{ID}$ indicates the internal diameter, $d$, for small bore pipes, the nominal diameter, $DN$, for valves, respectively; for the longitudinal body blockage (Fig. 4) the size of the annulus of the opening area, $R_{AN}$, and the diameter of the internal blockage (= 84.85 mm) characterize completely the device. Moreover, the wall thickness of all small bore pipes is $e_{ID} = 3.9$ mm. As indicated in Table 2, the difference between

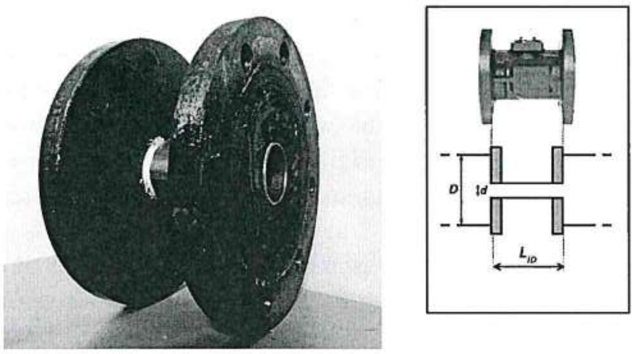


(a) (b)

Figure 3: Very short blockage (VSB): a) device; b) longitudinal-section (schematic).

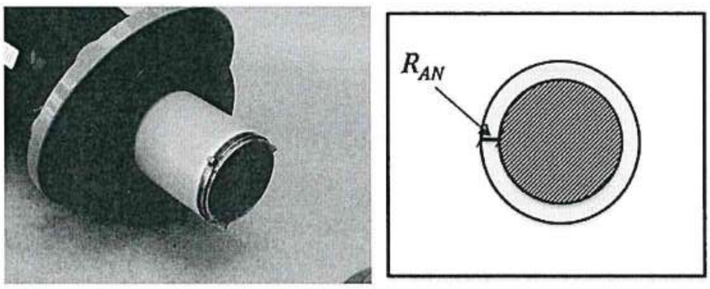


(a) (b)

Figure 4: Longitudinal body blockage (LB): a) device; b) cross-section (schematic).

Table 1: Main characteristics of discrete partial blockages used in the experiments.

| ID Type | $L_{ID}$ (mm) | $D_{ID}$ (mm) |
|---|---|---|
| Butterfly valve (BTV) | 60 | 100 |
| Ball valve (BV) | 120 | 90 |
| Small bore pipe (SBP) | 480 | 38.8 |
| Very short blockage (VSB) | 120 | 38.8 |
| Longitudinal body blockage (LB) | 480 | 4.22 |

the small bore pipe (SBP) and the very short blockage (VSB) is given by $L_{ID}$, with the length of VSB being equal to that of the ball valve, BV (Fig. 3b). Similarly, the same blockage severity of the SBP results for the longitudinal body blockage (LB) but with the opening area of an annular shape (Fig. 4b).

The steady-state behavior of the devices simulating blockages is given by the value of the local head loss coefficient, $\chi_{ID}$, defined by the Borda equation: $\zeta_{ID,0} = \chi_{ID}\ V_0^2/(2g)$, with $g$ = gravity acceleration; $\chi_{ID}$ values take into account also the friction losses through the blockage and are obtained by means of steady-state tests. In Fig. 5 such values are reported vs. the pre-transient Reynolds number, $Re_0 = V_0 D/\nu$, for given values of the opening degree, $\delta_{ID}$ (= ratio between the blockage cross-sectional area and pipe area). The curves in Fig. 5 confirm that in turbulent flow regime the value of $\chi_{ID}$ – and thus the local energy dissipation – depends strongly on the flow path through the device. In fact, Fig. 5 shows that different devices with the same value of $\delta_{ID}$ but different geometrical characteristics exhibit a different steady-state behavior. As it will be shown below, the same applies to the transient response of such devices: for a given incident pressure wave, the reflected one depends on the characteristics of the path of pressure waves through them.

## 3. Laboratory Results and Discussion

### *3.1. Effect of the blockage geometrical characteristics on transient response*

Tests executed by Meniconi et al. (2011a) to analyze the transient behavior of a partially closed in-line valve show that $y_{ID}$, which is the pressure rise due to the arrival at the measurement section of the wave reflected by

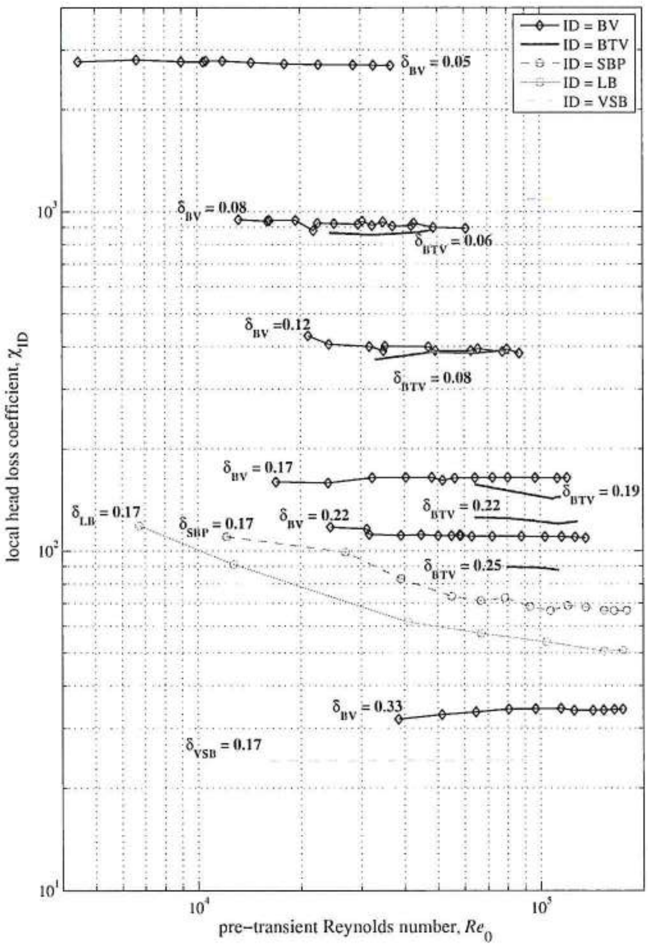


Figure 5: Local head loss coefficient, $\chi_{ID}$, vs. pre-transient Reynolds number, $Re_0$, for different blockage features and given opening degrees, $\delta_{ID}$ (ball valve (BV), butterfly valve (BTV), small bore pipe (SBP), longitudinal body blockage (LB), very short blockage (VSB)).

the blockage, depends on: i) $\zeta_{ID,0}$, ii) the distance between the in-line device and the measurement section (for the considered case, $L_2$), and iii) the clear pipe material (through the value of its pressure wave speed, $a$). It is worth noting that $L_2$ has no influence on the mechanism of interaction between the pressure waves and the device. However, it has to be taken into account when the transient behavior of the device is examined by measuring pressure waves at a certain distance from it. In fact, the larger $L_2$, the larger the damping of pressure waves due to viscoelasticity and friction. On the contrary, neither the opening area nor the pre-transient flow condition, i.e. $Re_0$, have a valuable effect on $y_{ID}$. In Meniconi et al. (2011a) it is shown that, for different types of valves but for a given value of $\zeta_{ID,0}$, $y_{ID}$ is the same irrespective of the value of $Re_0$. During tests, attention was focused on the first characteristic time of the pipe, $\tau = 2L/a$, in order to capture the first pressure wave reflected by the device. In fact, in the successive phases of the transients, the effect of the blockage is less and less distinguishable because of the overlapping of the pressure waves generated at the supply tank and by now closed downstream maneuver valve. Moreover, in the long term the effect of the blockage on the pressure signal is hidden by friction and viscoelasticity.

With the crucial role of $\zeta_{ID,0}$, in this paper the possible effect of the geometrical characteristics of the blockage, and thus the path of the pressure waves through it, is examined.

As discussed below, the results of the tests have pointed out that during $\tau$ the pressure signal may exhibit two different behaviors due to the mechanism of interaction between the incident pressure wave and the device: the first is characterized by a rise followed by an almost constant value (type I), whereas in the second a drop occurs after the rise (type II).

The first series of the laboratory tests concerns the comparison between two typical artificial blockages: ball (BV) and butterfly (BTV) valves (Fig. 6) with the same $\zeta_{ID,0}$ (= 5.37 m for case "a", and 9.91 m for case "b"); in the figures $t$ is the time evaluated since the beginning of the valve maneuver. Notwithstanding the very different value of $\delta_{ID}$, due to the characteristics of the body valve (a disk for the BTV and a ball for the BV), $y_{ID}$ is the same (= 4.48 m for case case "a" and 8.22 m for case "b") as well as the whole pressure signal behavior which is almost constant during $\tau$ after the rise $y_{ID}$. A similar behavior can be ascribed to the fact that since the path of pressure waves through these devices has almost the same characteristics (sinuous because of the body valve) the same is also the mechanism of interaction.

The aim of the second series of tests (Fig. 7) is to compare the mechanism of interaction of pressure waves with a ball valve (BV) and a very short

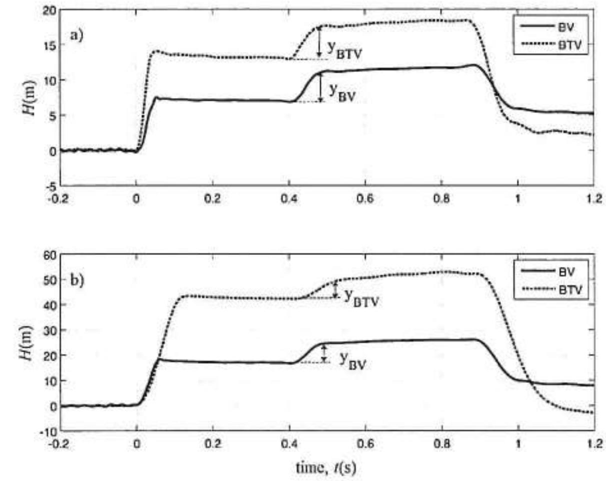


Figure 6: Experimental pressure signals for the butterfly valve (BTV) and ball valve (BV) – type I: a) $\zeta_{ID}$ = 5.37 m, $y_{ID}$ = 4.48 m; BV: $\delta_{BV}$ = 0.047, $Re_0$= 17111; BTV: $\delta_{BTV}$ = 0.056, $Re_0$= 32829; b) $\zeta_{ID}$ = 9.91 m, $y_{ID}$ = 8.22 m; BV: $\delta_{BV}$ = 0.082, $Re_0$= 42813; BTV: $\delta_{BTV}$ = 0.193, $Re_0$= 108831.

blockage (VSB) with the same $\zeta_{ID,0}$ (=1.17 m), $L_{ID}$ (= 120 mm), and $\delta_{ID}$ (= 0.17). Fig. 7 points out that $y_{ID}$ is the almost same (= 1.09 m), but a successive sudden drop can be observed in the very short blockage (VSB) – type II mechanism – with respect to the ball valve (BV) where the pressure signal remains constant – type I mechanism.

The fact that the path of pressure waves through the blockage influences the transient response is confirmed by Fig. 8 plots where the small bore pipe (SBP) and longitudinal body blockage (LB) are compared. Such blockages have the same $L_{ID}$ (= 480 mm), the same opening degree ($\delta_{ID}$ = 0.17), as well as the same $\zeta_{ID,0}$ (= 0.51 m). More importantly, the path of pressure waves is almost straight in both cases, and, as a result, the whole transient response is the same.

Based on the above experiments, it can be stated that the path of pressure waves through the device plays a crucial role in the mechanism of interaction with pressure waves during the pipe first characteristics time: sinuous through the valves, because of the presence of the body valve (type I), and almost rectilinear through the very short blockage, small bore pipe, and longi-

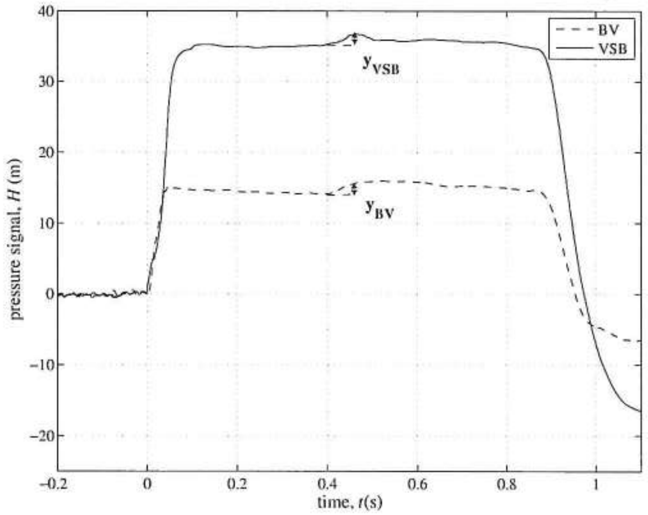


Figure 7: Experimental pressure signals for the ball valve (BV) – type I – and very short blockage (VSB) – type II – ($\zeta_{ID}$ = 1.17 m, $\delta_{ID}$ = 0.17, $y_{ID}$ = 1.09 m; BV: $Re_0$= 35260; VSB: $Re_0$= 90573).

tudinal body blockage (type II), because of their constant longitudinal shape. To better understand laboratory pressure traces of Figs. 6 to 8, some numerical experiments have been executed concerning – for the sake of simplicity – the case of the frictionless elastic pipe, with the same geometrical characteristics of the laboratory setup, where an instantaneous maneuver generates a single pressure wave, $\Delta H_I$. For the short stretches of pipe with a reduced diameter, numerical simulations assume that during transients a gradually varied flow takes place between the downstream (DC) and the upstream connection (UC) between the clear pipe and the blockage (Fig. 9). With regard to valves, the effect of the local head loss is taken into account since it dominates the mechanism of interaction. In the below plots, the dimensionless pressure signals

$$h = \frac{H - H_0}{\Delta H_{AJ}} \tag{1}$$

are considered, with $\Delta H_I = \Delta H_{AJ} = \frac{aV_0}{g}$ being the Allievi-Joukowski overpressure.

As an example of type II mechanism, in the case of the small bore pipe (SBP),

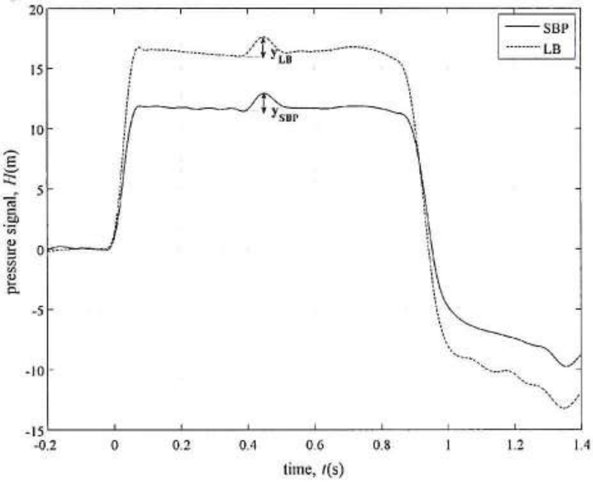


Figure 8: Experimental pressure signals for the SBP and LB (type II) ($\zeta_{ID}$ = 0.51 m, $\delta_{ID}$ = 0.17, $y_{ID}$ = 1.03 m; SBP: $Re_0$= 27044; LB: $Re_0$= 40984).

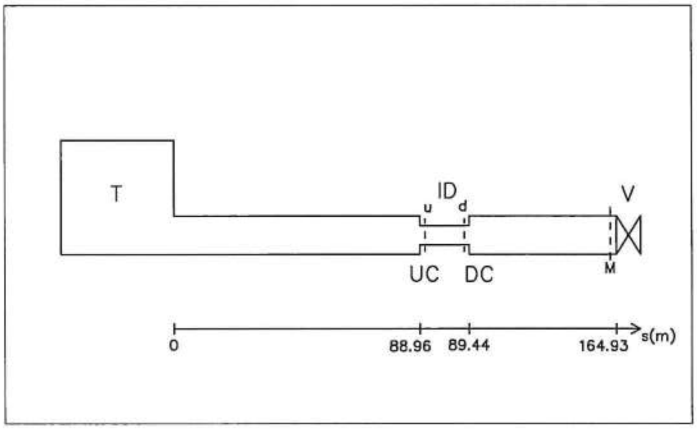


Figure 9: The small bore pipe system – SBP (T = supply tank; UC, DC = upstream, downstream connection between the blockage and the clear pipe; ID = in-line device; u,d = computational sections; M = measurement section; and V = maneuver valve).

at $t_1 = L_2/a$, $\Delta h_I$, as an incident pressure wave (Fig. 10a), approaches the downstream connection (DC) and gives rise to the reflected wave, $\Delta h_R^{(1)}$, which propagates back towards the downstream end section, and transmitted wave, $\Delta h_T^{(1)}$, (Fig. 10b) which travels towards the upstream connection (UC). At $t_2 = t_1 + L_{ID}/a_{ID}$, with $a_{ID}$ = pressure wave speed of the SBP, $\Delta h_T^{(1)}$ interacts with the upstream connection (UC) and generates a second couple of waves: the reflected pressure wave, $\Delta h_R^{(2)}$, proceeding back towards the DC, and the transmitted pressure wave, $\Delta h_T^{(2)}$, traveling along the upstream branch of pipe (Fig. 10c). On the contrary, $\Delta h_R^{(1)}$ will affect again the small bore pipe only at time $t = t_1 + 2L_2/a$, after it has been reflected back by the now closed maneuver valve. At $t_3 = t_2 + L_{ID}/a_{ID}$, $\Delta h_R^{(2)}$ reaches

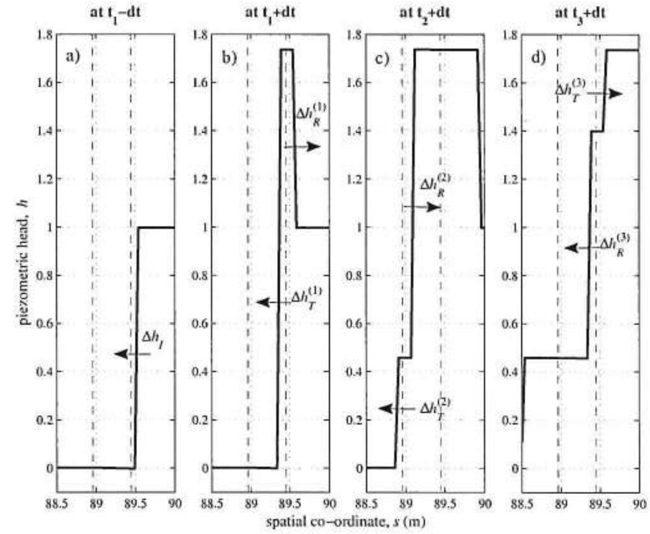


Figure 10: Sketch of the reflected and transmitted dimensionless numerical pressure waves at the small bore pipe device, generated by a single incident pressure wave, $\Delta h_I$, in a frictionless elastic pipes at some distinctive instants of time during the pipe first characteristic time.

the DC and it is reflected back towards UC, as $\Delta h_R^{(3)}$, and transmitted towards the end section, as $\Delta h_T^{(3)}$ (Fig. 10d). On the contrary, the effects of $\Delta h_T^{(2)}$ on the small bore pipe will occur only at $t = t_2 + 2L_1/a$. Then $\Delta h_R^{(3)}$ behaves as $\Delta h_T^{(1)}$ and the interaction between the pressure waves and the SBP proceeds during the first characteristic time giving rise to smaller and smaller pressure waves inside the SBP. In Fig. 11 the dimensionless pressure signal at sections "d" and "u" (the former just upstream of DC and the latter just downstream of UC) shows the progressive decay caused by the above mechanism of interaction. At the measurement section M of the

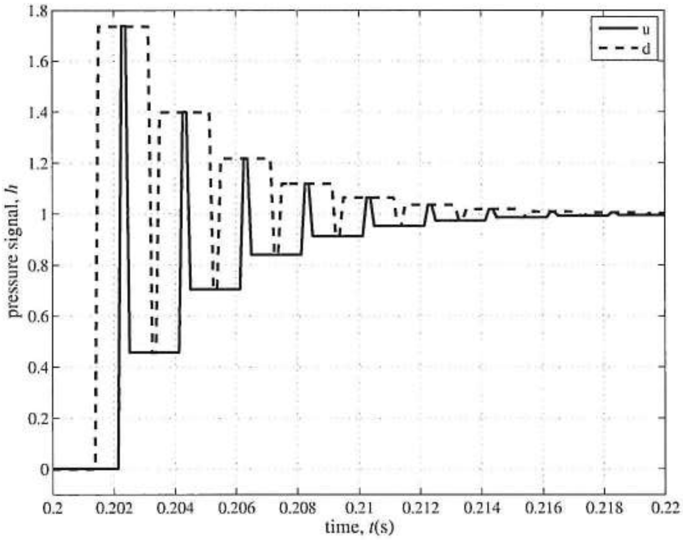


Figure 11: Decay of dimensionless numerical pressure signal inside the small bore pipe (SBP) after the arrival of a single incident pressure wave in a frictionless elastic pipe.

laboratory experiments the above interaction between pressure waves and SBP results in a sort of terrace-shape curve which is the distinctive feature of a SBP placed at a certain distance upstream when a single pressure wave is generated at M. At this section, the effect of a maneuver with a duration $T$, which generates a pressure wave train and not a single wave, is a huge smoothing and a delay in time of the pressure traces as shown in Fig. 12 where different values of $T$ (= 0 s, 0.05 s and 0.1 s) are considered.

A completely different phenomenon happens when the incident pressure wave, $\Delta h_I$, interacts with a butterfly valve: a single reflected pressure wave, $\Delta h_R^{(1V)}$, is produced since the transmitted pressure wave, $\Delta h_T^{(1V)}$, travels along the upstream branch of pipe with no interaction with any singularity. This is the reason why the pressure trace at section M shows a single rise and is almost constant until the arrival of the second pressure wave reflected by the in-line valve.

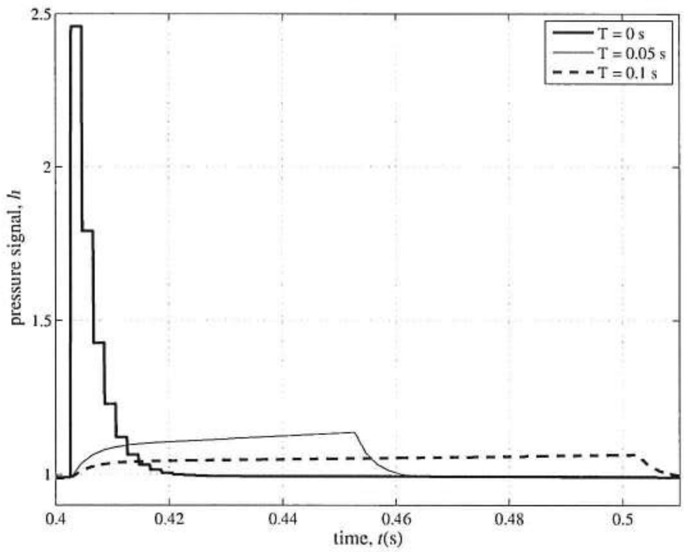


Figure 12: The effect of the duration, $T$, of the maneuver generating the pressure waves on the dimensionless pressure signal at the measurement section M in a frictionless elastic pipe with a small bore pipe device.

### *3.2. Effect of the pre-transient conditions for blockages of type II*

The fourth series of laboratory experiments concerns the transient behavior of discrete blockages of type II with regard to the possible effect of the pre-transient conditions – i.e., $Re_0$, and thus $\zeta_{ID,0}$ – in order to fill such a gap with respect to type I devices examined in Meniconi et al. (2011a). In Figs. 13 and 14 pressure signals with increasing $Re_0$ are shown for the very short blockage (VSB) and the small bore pipe (SBP), respectively. In both cases, for the smaller values of $Re_0$, the mechanism of interaction of pressure waves is of type II, according to the experiments discussed above. Then, the larger $Re_0$, and thus $\zeta_{ID,0}$, the more the transient response fits in with type I (Figs. 13b and 14b).

To explore in more details such a behavior, numerical experiments have been executed by considering the laboratory pipes. The used 1-D model – described in Appendix I – is based on the method of characteristics and unsteady friction, viscoelasticity, and the minor head loss at both the sudden contraction and enlargement are taken into account (Idel'cik, 1986). Moreover, it is assumed that a gradually varied flow takes place in both the small

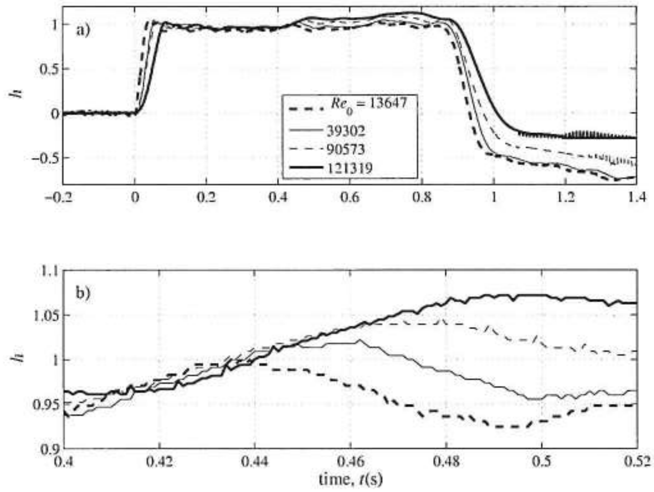


Figure 13: Dimensionless experimental pressure signals for the very short blockage (VSB) with different values of $Re_0$: a) in the first characteristics time $= 2L/a$; b) magnified vision in the time interval when most of the interaction between pressure waves and the device takes place.

bore pipe (SBP), and the very short blockage (VSB). It is worth noting that the performance of this model has been extensively checked with good results for different systems: a single pipe (Meniconi et al., 2012b), a pipe with: a partially closed in-line valve (Meniconi et al., 2012b), a discrete and extended blockage (Meniconi et al., 2012a, 2014), and a leak (Meniconi et al., 2013a). To compare the experimental and numerical pressure traces, the root mean square error, $\epsilon = \sqrt{\frac{\sum_{i=1}^{N}(H_n-H)^2}{N}}$, is evaluated, with $N$ = number of samples in the first characteristic time, and the subscript $n$ indicating the numerical model outcome. In Fig. 15, as an example, the behavior of $\epsilon$ vs. $Re_0$ is shown for the small bore pipe device (SBP). The discrepancies between numerical and laboratory results can be ascribed mainly to the failure of the assumed hypothesis of a gradually flow along the device. Moreover, the curves of this figure show that $\epsilon$ increases if the minor head loss at the contraction and enlargement are not taken into account. However, even if the effect of such local head losses is not negligible, they do not play a crucial role in the simulation of the phenomenon. A further check has concerned, as an example, the test with the largest $Re_0$ (Fig. 16). The curves in this figure confirm

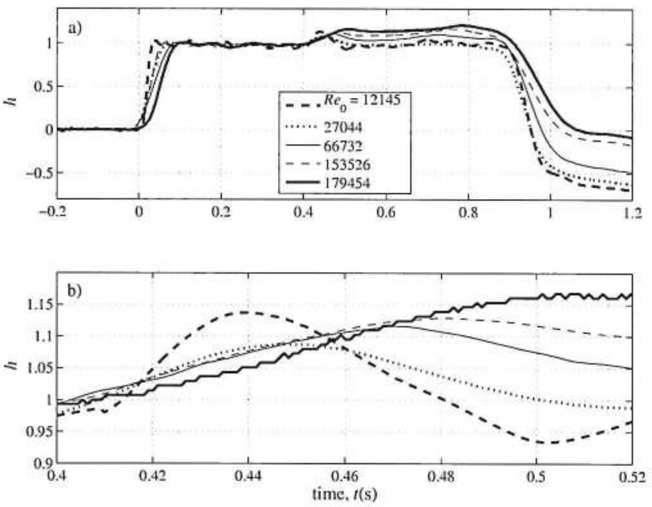


Figure 14: Dimensionless experimental pressure signals for the small bore pipe (SBP) with different values of $Re_0$: a) in the first characteristics time $= 2L/a$; b) magnified vision in the time interval when most of the interaction between pressure waves and the device takes place.

that the quality of the numerical simulation increases if the local head losses at UC and DC are considered; however, it definitely improves by assuming a type I mechanism. In other words, the value of $\epsilon$ decreases if it is assumed that the small bore pipe behaves as a partially closed in-line valve with, as a unique local head loss, the one measured in the steady-state condition.

To better highlight the evolution of type II mechanism towards the type I behavior, parallels can be drawn with the so called Eytelwein phenomenon. Such a phenomenon happens in steady-state condition (Eytelwein, 1801; Arredi, 1934) when the distance between two orifices in series decreases and the global effect – i.e., the total local head loss – is no more given by the sum of two distinct energy dissipations since the second orifice interacts with the flow downstream of the first one. Mutatis mutandis, the carried out experiments show that a similar phenomenon happens in transient conditions: when $Re_0$ increases, the two distinct minor head losses at the sudden contraction and enlargement collapse into a unique energy dissipation and the transient behavior is equal to the one of a partially closed in-line valve (type I mechanism). For the special case of no initial flow (i.e., $Re_0 = 0$), the

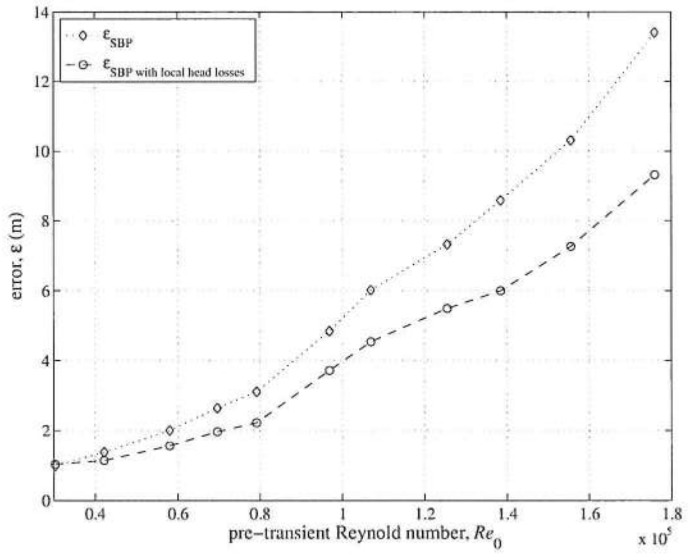


Figure 15: Root mean square error of the numerical model, $\epsilon$, vs. pre-transient Reynolds number, $Re_0$, when the flow through SBP is assumed as gradually varied.

pressure wave must be generated by a specific pressure wave maker device as the one described in Brunone et al. (2008b). In such a case, different boundary conditions apply and a different mechanism of interaction happens as discussed in details in Meniconi et al. (2011b).

## 4. Conclusions

In this paper the mechanism of interaction of pressure waves and discrete blockages has been analyzed in detail. A huge amount of laboratory experiments has been carried out at the Water Engineering Laboratory of the University of Perugia, Italy, with different types of discrete blockages: a butterfly and a ball valve, two small bore pipes and a longitudinal body blockage.

Based on previous results for a partially closed in-line valve (Meniconi et al., 2011a), in the first phase of the experimental campaign, transients with the same steady-state local head loss at the in-line device, $\zeta_{ID,0}$, but very different geometrical characteristics, have been considered. These tests have confirmed the crucial role of $\zeta_{ID,0}$ and pointed out that two mechanisms of

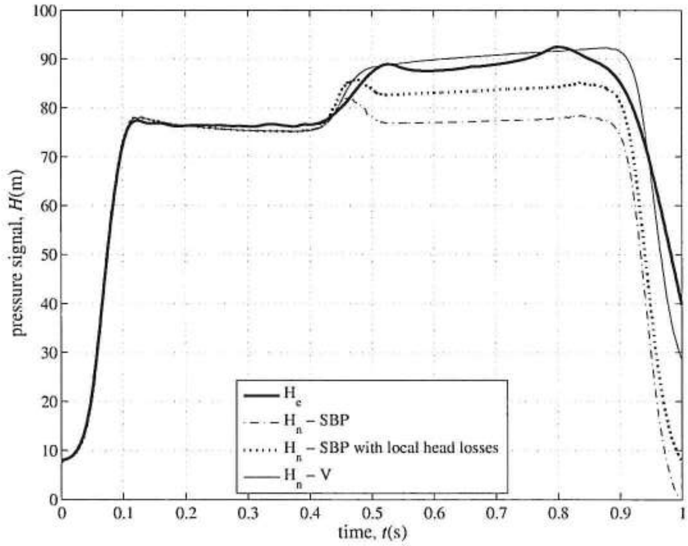


Figure 16: Experimental (bold line) vs. numerical pressure signals for different mechanisms of interaction at the small bore pipe (SBP), for the largest value of $Re_0$ (= 179454): the dash-dotted and the bold dotted line indicates type II numerical trace without and with local head losses at UC and DC, respectively; the thin continuous line indicates type I numerical trace.

interaction with the pressure waves can occur. The type I mechanism happens when the path of the pressure waves is sinuous, as through a partially closed in-line valve, whereas the type II mechanism takes place at a small bore pipe where the path of pressure waves is almost straight. The differences between type I and type II mechanisms influence the pressure signal: for a given $\zeta_{ID,0}$, the same first pressure rise occurs, whereas a successive drop takes place only for type II mechanism. To better understand laboratory pressure traces, numerical experiments have been carried out to analyze the interaction of pressure waves with the blockages and examine the effect of maneuver duration.

Further numerical and laboratory experiments carried out on the small bore pipe (SBP) and the very short blockage (VSB) show that the type II mechanism of interaction is affected by the pre-transient flow condition. Precisely, the larger the pre-transient Reynolds number, and thus the local head loss, the more the type II behavior evolves towards the type I one. This phenomenon may be ascribed to the fact that only for the smallest values of $Re_0$

a gradually varied flow takes place throughout the device and two distinct local head losses happen at the sudden constriction and enlargement, respectively. In other words, when $Re_0$ increases, such minor head losses give rise to a unique energy dissipation as a partially closed in-line valve (type I mechanism). Thus it can be affirmed that for type II blockages the mechanism of interaction with pressure waves is a sort of dynamic behavior, according to pre-transient condition. Such a result has been confirmed by the outcomes of the 1-D numerical model simulating transients in viscoelastic pipes with a discrete blockage.

## Appendix I – Numerical model

According to literature (Covas et al., 2005; Franke and Seyler, 1983; Ghilardi and Paoletti, 1986; Keramat et al., 2012; Meniconi et al., 2012a,b; Soares et al., 2008), the complete 1-D model to simulate transients in pressurized viscoelastic pipes is based on the continuity:

$$\frac{\partial H}{\partial t} + \frac{a^2}{g}\frac{\partial V}{\partial s} + \frac{2a^2}{g}\frac{d\epsilon_r}{dt} = 0, \tag{2}$$

and momentum equation:

$$\frac{\partial H}{\partial s} + \frac{V}{g^2}\frac{\partial V}{\partial s} + \frac{1}{g}\frac{\partial V}{\partial t} + J = 0, \tag{3}$$

with $J$ = total friction term ($= 4\tau_w/\rho g D$), $\tau_w$ = wall shear stress, $\rho$ = fluid density, and $s$ = spatial co-ordinate. These equations are integrated numerically within the method of the characteristics.

In this paper a single element Kelvin-Voigt model is used, i.e. a viscous damper and an elastic spring are connected in parallel and joined to a simple elastic spring in series. Thus, the third term of Eq. (2) is described by the following relationship:

$$\sigma = E_r\epsilon_r + \frac{E_r}{T_r}\frac{d\epsilon_r}{dt}, \tag{4}$$

where $\sigma$ = circumferential stress ($= \psi p D/2e$, with $\psi$ = dimensionless parameter that takes into account pipe size and constraints, and $p$ = internal pressure), $E_r$ = dynamic modulus of elasticity, and $T_r$ = retardation time of the viscous damper of the Kelvin-Voigt element. The elastic strain, $\epsilon_{\mathrm{el}}$, of the spring is given by:

$$\epsilon_{\mathrm{el}} = \frac{\sigma}{E_{\mathrm{el}}}, \tag{5}$$

where $E_{\mathrm{el}}$ = the elastic Young's modulus of elasticity. According to literature, $\tau_w$ is regarded as the sum of two components:

$$\tau_w = \tau_{w,s} + \tau_{w,u}, \tag{6}$$

where the subscripts $s$ and $u$ indicate the steady- and unsteady-state component, respectively. In this paper, $\tau_{w,u}$ is evaluated by means of an instantaneous acceleration-based model (Ghidaoui et al., 2005):

$$\tau_{w,u} = \frac{\rho k_{uf} D}{4}\left(\frac{\partial V}{\partial t} + \mathrm{sign}\left(V\frac{\partial V}{\partial s}\right) a\frac{\partial V}{\partial s}\right), \tag{7}$$

where $k_{uf}$ = unsteady friction coefficient, and $\mathrm{sign}(V\partial V/\partial s) = (+1$ for $V\partial V/\partial s \geq 0$ or $-1$ for $V\partial V/\partial s < 0)$. Model parameters (i.e., $E_{\mathrm{el}}$, $E_r$, and $T_r$) have been calibrated by considering transients in single pipes by minimizing the difference between numerical and experimental pressure signals whereas $k_{uf}$ is evaluated following the procedure described in (Pezzinga, 2000). Then, the so-obtained values of parameters have been exported and tested on the in-line valve pipe (Meniconi et al., 2012b), in series pipes (Meniconi et al., 2012a), and leaky pipe (Meniconi et al., 2013a). The resulting values of the model parameters are: $E_{\mathrm{el}} = 2.20 \cdot 10^9$ N/m$^2$, $a = 377.15$ m/s, $E_r = 8.50 \cdot 10^9$ N/m$^2$, $T_r = 0.13$ s for the clear pipe, $E_{\mathrm{el,ID}} = 2.62 \cdot 10^9$ N/m$^2$, $a_{ID} = 431.38$ m/s, $E_{r,ID} = 15.0 \cdot 10^9$ N/m$^2$, $T_{r,ID} = 0.08$ s for the small bore pipe. The boundary conditions at the supply tank and in-line and maneuver valve are described in details in (Meniconi et al., 2012b).

## Acknowledgements

This research is funded by the University of Perugia, Italian Ministry of Education, University and Research (MIUR) – under the Projects of Relevant National Interest "Advanced analysis tools for the management of water losses in urban aqueducts" and "Tools and procedures for an advanced and sustainable management of water distribution systems" – and Fondazione Cassa Risparmio Perugia, under the project "Hydraulic and microbiological combined approach towards water quality control (no. 2015.0383.021)".

## References

Adewumi, M. A., Eltohami, E. S., Ahmed, W. H., 2000. Pressure transients across constrictions. J. Energy Resour. Technol. 122, 34–41.

Adewumi, M. A., Eltohami, E. S., Solaja, A., 2003. Possible detection of multiple blockages using transients. J. Energy Resour. Technol. 125, 154–159.

Arredi, F., 1934. Ricerche sperimentali sul fenomeno di Eytelwein (in Italian). Ricerche di Ingegneria 6, 1–21.

Boulos, P. F., Lansey, K. E., Karney, B. W., 2006. Comprehensive Water Distribution Systems Analysis Handbook for Engineers and Planners, 2nd Edition. MWH SOFT, Pasadena, CA.

Brunone, B., Ferrante, M., Meniconi, S., 2008a. Discussion of "Detection of partial blockage in single pipelines" by P.K. Mohapatra, M.H. Chaudhry, A.A. Kassem, and J. Moloo. J. Hydraul. Eng. 134 (6), 872–874.

Brunone, B., Ferrante, M., Meniconi, S., 2008b. Portable pressure wave-maker for leak detection and pipe system characterization. J. Am. Water Work Assoc. 100 (4), 108–116.

Chaudhry, M. H., 2014. Applied Hydraulic Transients, 3rd Edition. Springer.

Contractor, D., 1965. The reflection of waterhammer pressure waves from minor losses. J. Basic Eng. 87, 445–451.

Covas, D., Stoianov, I., Mano, J., Ramos, H., Graham, N., Maksimovic, C., 2005. The dynamic effect of pipe-wall viscoelasticity in hydraulic transients. Part II - model development, calibration and verification. J. Hydraul. Res. 43 (1), 56–70.

Douterelo, I., Boxall, J. B., Deines, P., Sekar, R., Fish, K. E., Biggs, C. A., 2014. Methodolgical approaches for studying the microbial ecology of drinking water distribution systems. Water Res. 65, 134–156.

Duan, H.-F., Lee, P. J., Ghidaoui, M. S., 2014a. Transient wave-blockage interaction in pressurized water pipelines. Procedia Engineering 89, 573–582.

Duan, H.-F., Lee, P. J., Ghidaoui, M. S., Tuck, J., 2014b. Transient wave-blockage interaction and extended blockage detection in elastic water pipelines. J. Fluids Struct. 46, 2–16.

Duan, H.-F., Lee, P. J., Ghidaoui, M. S., Tung, Y.-K., 2012. Extended blockage detection in pipelines by using the system frequency response analysis. J. Water Resour. Plan. Manage. 138 (1), 55–62.

Duan, H.-F., Lee, P. J., Kashima, A., Lu, J., Ghidaoui, M. S., Tung, Y.-K., 2013. Extended blockage detection in pipes using the system frequency response: analytical analysis and experimental verification. J. Hydraul. Eng. 139 (7), 763–771.

Duan, H.-F., Lee, P. J., Tuck, J., 2014c. Experimental investigation of wave scattering effect of pipe blockages on transient analysis. Procedia Engineering 89, 1314–1320.

Eytelwein, J. A., 1801. Handbuch der Mechanik und der Hydraulik. F.L. Lagarde, Berlin.

Franke, P., Seyler, F., 1983. Computation of unsteady pipe flow with respect to visco-elastic material properties. J. Hydraul. Res. 21 (5), 345–353.

Ghidaoui, M., Zhao, M., McInnis, D., Axworthy, D., 2005. A review of water hammer theory and practice. Appl Mech Rev 58 (1), 49–76.

Ghilardi, P., Paoletti, A., 1986. Additional visco-elastic pipes as pressure surges suppressors. In: Proc. 5th Intl. Conf. Pressure Surges, Cranfield (UK). pp. 113–121.

Idel'cik, I. E., 1986. Handbook of Hydraulic Resistance. Hemisphere publishing corp, New York.

Karney, B. W., 1990. Energy relations in transient closed-conduit flow. J. Hydraul. Eng. 116 (10), 1180–1196.

Keramat, A., Tijsseling, A. S., Hou, Q., Ahmadi, A., 2012. Fluid-structure interaction with pipe-wall viscoelasticity during water hammer. J. Fluids Struct. 28, 434–455.

Lee, P. J., Duan, H.-F., Ghidaoui, M. S., Karney, B. W., 2013. Frequency domain analysis of pipe fluid transient behaviour. J. Hydraul. Res. 51 (6), 609–622.

Lee, P. J., Vitkovsky, J. P., 2008. Discussion of "Detection of partial blockage in single pipelines" by P.K. Mohapatra, M.H. Chaudhry, A.A. Kassem, and J. Moloo. J. Hydraul. Eng. 134 (6), 874–876.

Lee, P. J., Vitkovsky, J. P., Lambert, M. F., Simpson, A. R., Liggett, J. A., 2008. Discrete blockage detection in pipelines using the frequency response diagram: numerical study. J. Hydraul. Eng. 134 (5), 658–663.

Massari, C., Yeh, T. C. J., Ferrante, M., Brunone, B., Meniconi, S., 2014. Detection and sizing of extended partial blockages in pipelines by means of a stochastic successive linear estimator. J Hydroinform 16 (2), 248–258.

Massari, C., Yeh, T. C. J., Ferrante, M., Brunone, B., Meniconi, S., 2015. A stochastic approach for extended partial blockage detection in viscoelastic pipelines: numerical and laboratory experiments. J. Water Supply: Res. Technol. - Aqua 64 (5), 583–595.

Massari, C., Yeh, T. C. J., Ferrante, M., Brunone, B., S Meniconi, S., 2013. Diagnosis of pipe systems by means of a stochastic successive linear estimator. Water Resour. Manage. 27 (13), 4637–4654.

Meniconi, S., Brunone, B., Ferrante, M., 2011a. In-line pipe device checking by short period analysis of transient tests. J. Hydraul. Eng. 137 (7), 713–722.

Meniconi, S., Brunone, B., Ferrante, M., 2012a. Water hammer pressure waves at cross-section changes in series in viscoelastic pipes. J. Fluids Struct. 33, 44–58.

Meniconi, S., Brunone, B., Ferrante, M., Massari, C., 2010. Potential of transient tests to diagnose real supply pipe systems: what can be done with a single extemporary test. J. Water Resour. Plan. Manage. 137 (2), 238–241.

Meniconi, S., Brunone, B., Ferrante, M., Massari, C., 2011b. Small amplitude sharp pressure waves to diagnose pipe systems. Water Resour. Manage. 25 (1), 79–96.

Meniconi, S., Brunone, B., Ferrante, M., Massari, C., 2012b. Transient hydrodynamics of in-line valves in viscoelastic pressurized pipes: long-period analysis. Exp. Fluids 53 (1), 265–275.

Meniconi, S., Brunone, B., Ferrante, M., Massari, C., 2013a. Numerical and experimental investigation of leaks in viscoelastic pressurized pipe flow. Drink. Water Eng. Sci. 6 (1), 11–16.

Meniconi, S., Brunone, B., Ferrante, M., Massari, C., 2014. Energy dissipation and pressure decay during transients in viscoelastic pipes with an in-line valve. J. Fluids Struct. 45, 235–249.

Meniconi, S., Duan, H.-F., Lee, P. J., Brunone, B., Ghidaoui, M. S., Ferrante, M., 2013b. Experimental investigation of coupled frequency- and time-domain transient test-based techniques for partial blockage detection in pipelines. J. Hydraul. Eng. 139 (10), 1033–1040.

Mohapatra, P., Chaudhry, M., Kassem, A., Moloo, J., 2006a. Detection of partial blockage in single pipelines. J. Hydraul. Eng. 132 (2), 200–206.

Mohapatra, P. K., Chaudhry, M. H., 2011. Frequency responses of single and multiple partial pipeline blockages. J. Hydraul. Res. 49 (2), 263–266.

Mohapatra, P. K., Chaudhry, M. H., Kassem, A., Moloo, J., 2006b. Detection of partial blockages in a branched piping system by the frequency response method. J. Fluids Eng. 128 (5), 1106–1114.

Pezzinga, G., 2000. Evaluation of unsteady flow resistances by quasi-2D or 1D models. J. Hydraul. Eng. 126 (10), 778–785.

Sattar, A. M., Chaudhry, M. H., Kassem, A. A., 2008. Partial blockage detection in pipelines by frequency response method. J. Hydraul. Eng. 134 (1), 76–89.

Soares, A., Covas, D., Reis, L., 2008. Analysis of PVC pipe-wall viscoelasticity during water hammer. J. Hydraul. Eng. 134 (9), 1389–1395.

Tuck, J., Lee, P. J., Davidson, M., Ghidaoui, M. S., 2013. Analysis of transient signals in simple pipeline systems with an extended blockage. J. Hydraul. Res. 51 (6), 623–633.

Wang, X., Lambert, M., Simpson, A., 2005. Detection and location of a partial blockage in a pipeline using damping of fluid transients. J. Water Resour. Plan. Manage. 131 (3), 244–249.

Yeh, T.-C., Jin, M., Hanna, S., 1996. An iterative stochastic inverse method: conditional effective transmissivity and hydraulic head fields. Water Resour. Res. 32 (1), 85–92.